Available online at www.sciencedirect.com
SCIENCE DIRECT
Solid State Communications 131 (2004) 47–51
solid state communications
www.elsevier.com/locate/ssc

The trapping centers of holes in a-As_2Se_3

P. Kounavis*

Department of Engineering Sciences, School of Engineering, University of Patras, Rio Patras, 26504 Patras, Greece

Received 11 August 2003; received in revised form 17 March 2004; accepted 14 April 2004 by D.E. Van Dyck

Abstract

The density of the trapping centers and their capture radius for holes in a-As_2Se_3 are determined by analyzing the imaginary term of the modulated photocurrent. The light-induced changes in the imaginary term are also examined to study the influences of the photo structural changes to the density of states and to detect possible hole trapping at light created charged defects.

PACS: 71.55.Jv; 73.50.Gr; 81.15.Cd

Keywords: A. Amorphous semiconductors; D. Electronic states (localized); D. Trapping and recombination

1. Introduction

Amorphous chalcogenides (e.g. Se, S, selenides or sulfides of Ge, As etc.) have attracted a great deal of interest as they represent many unique properties [1]. These properties have been successfully explained by incorporating native defect states in the density of states (DOS), which are characterized by negative effective correlation energy [2]. It was postulated that these defects occur in concentration of $10^{17}-10^{19}cm^{-3}$ and arise from under- and over-coordinated atoms (i.e. As and Se atoms in a-As_2Se_3), respectively, well-known as valence alternation pairs (VAPs) [3]. Recent data from extended X-rays absorption fine-structure (EXAFS) [4,5], Raman scattering [6] and electron spin resonance (ESR) [7] experiments in amorphous chalcogenides are consistent with the VAP model. The ESR experiments during or after illumination provided an unpaired spin density of $10^{20}cm^{-3}$ that was attributed to the VAPs [7].

The importance of the VAP model has been recently questioned by Tanaka [8]. Based on optical absorption measurements the above author argued that wrong bonds (i.e. As–As) are more important defects governing the macroscopic electronic properties. Moreover, the distributions of the defect states of the VAP model have not been manifested by conventional spectroscopic techniques of the DOS, like transient photocurrent (TPC) [9–11] and modulated photocurrent (MPC) [12,13] experiments. These experiments revealed usually featureless exponential DOS. The nature of this DOS is still not known. In contrast, steady state photoconductivity indicates that recombination of holes takes place at well-defined energy levels [14,15].

In a recent comparative analysis of the imaginary and real term of the MPC of a-As_2Se_3 [16] it was deduced that apart from the exponential tail, which is usually extracted from TPC and MPC experiments, there are additional gap states that act as deep trapping and recombination centers for holes. These centers were found using bias illumination and may dominate steady state photoconductivity. In this paper, we concentrated on the characteristics of the DOS of the trapping centers of a-As_2Se_3 with which the majority carriers interact through trapping and thermal release as resulted from the analysis of the imaginary term of the MPC. The light-induced changes in the imaginary term are also studied to examine the influences of the photostructural changes on the DOS and their capture radius. Our analysis [17] was recently applied in a-Si:H and proved sensitive to resolve contributions from different gap states even when their relative density is quite different [18]. That analysis is also applied here to examine whether there is a thermal

* Tel.: +30-261-099-6281; fax: +30-261-099-6260.
E-mail address: pkounavis@des.upatras.gr (P. Kounavis).

0038-1098/$ - see front matter © 2004 Elsevier Ltd. All rights reserved.
doi:10.1016/j.ssc.2004.04.018

interaction of holes with native or light-created charged defects [7] of the VAP model.

2. Details of the experiment and analysis

The a-As_2Se_3 films with a thickness of 0.85 μm have been deposited by rf sputtering [19]. Before measurements, the samples were annealed for 4 h at 450 K to obtain the annealed (A) state. A 50 mW/cm^2 white filtered light from a halogen lamp was used to study the light-induced changes. The phase shift ϕ and amplitude of the MPC i_{ac} were measured as a function of the angular modulation frequency ω using a lock-in amplifier. For the MPC measurements a modulated red light from a light emitted diode with a maximum intensity at 660 nm was used [13,19]. All the measurements were conducted keeping the sample under vacuum.

It is assumed that the holes, which are the majority carriers, interact with the gap states below the Fermi level E_F through trapping and thermal release [9]. In general, we consider several kinds (i) of such gap state distributions $D^i(E)$ each one with a capture coefficient c_p^i for holes. The imaginary term Y of the MPC calculated by means of ϕ, i_{ac} is directly related to the various $D^i(E)$ through [17]

$$Y = \mu e G_{ac} A \varepsilon \frac{\sin\phi}{i_{ac}} \cong \frac{\pi}{2} \sum_i H^i(\omega_t^i, \omega) c_p^i D^i(E_\omega^i) kT. \qquad (1)$$

In Eq. (1), μ is the mobility of holes, e the electronic charge, G_{ac} the amplitude of the alternating generation rate, A the conduction cross sectional area of the specimen, kT the thermal energy and ε the applied electric field. Each probing energy level E_ω^i is given by $E_\omega^i = kT \ln[(c_p^i N_V)/(\omega^2 + \{\omega_t^i\}^2)^{1/2}]$, where N_V is of the order of 10^{20} cm^{-3} and represents the effective density of states in the valence band edge where the zero point of the energy scale is taken. The product $c_p^i N_V$ is the attempt to escape frequency, which is of the order of 10^{12}–10^{13} s^{-1}.

Every transition frequency ω_t^i corresponds to the quasi Fermi level E_{tp} of trapped holes and can be approximated by $\omega_t^i \cong pc_p^i$, where p is the density of free holes. In Eq. (1), the weighting function $H^i(\omega_t^i, \omega)$, hereafter H function, determines every effective contribution of the trapping rate $c_p^i D^i(E_\omega^i) kT$ to the imaginary term and is given by

$$H^i(\omega_t, \omega) = 1 - \frac{2}{\pi} \arctan\left(\frac{\omega_t^i}{\omega}\right). \qquad (2)$$

3. Experimental results and analysis

The imaginary terms Y_0, Y_0' and Y calculated from Eq. (1) by means of the respective experimental i_{ac}, ϕ data measured at 293 K for two relatively weak (F_0 and F_0') and moderate (F) bias illumination levels are shown in Fig. 1.

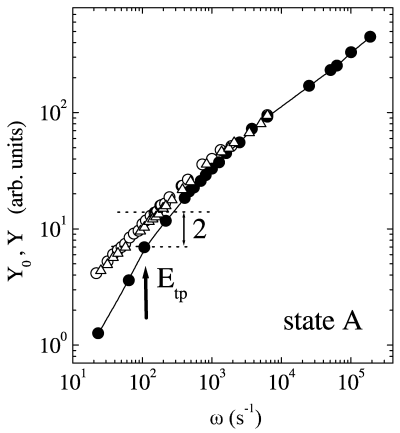

Fig. 1. Imaginary terms Y_0 (open circles), Y_0' (open triangles) and Y (closed circles) for two weak $F_0 = 8.2 \times 10^{11}$ cm^{-2} s^{-1}, $F_0' = 3.6 \times 10^{12}$ cm^{-2} s^{-1} and moderate $F = 2.8 \times 10^{13}$ cm^{-2} s^{-1} bias light intensities, respectively, at 293 K as a function of angular modulation frequency ω.

The values of Y_0 and Y_0' of Fig. 1 measured with the two weak bias-light levels (F_0 and F_0') and the respective values of Y at higher frequencies measured with the moderate bias-light level (F) are practically independent of the bias light intensity. This defines the emission-limited regime [17] which occurs for $\omega_t^i \ll \omega$ so that $H^i(\omega_t^i, \omega) \cong 1$.

In the respective spectrum of Y with the moderate bias light level (F) a drop takes place with a frequency dependence very similar to that of the H function from Eq. (2), which defines the trapping-limited regime [17]. This can be taken as an indication that a single kind of gap states probably dominates the imaginary term. In this case, Eq. (1) is reduced to $Y \cong (\pi/2) H(\omega_t, \omega) c_p D(E_\omega) kT$ and the spectral shape of Y term is determined from the DOS distribution and the spectral shape of H function. Thus the net drop of Y from the decrease of the respective $H(\omega_t, \omega)$ function should be obtained by dividing the Y values with the respective Y_0 values of the same trap depth. This is because Y_0 values correspond to the emission-limited regime, that takes place for $\omega_{t0} \ll \omega$ such that $H(\omega_{t0}, \omega) \cong 1$, therefore, we should obtain $Y/Y_0 = H(\omega_t, \omega)$. For the calculation of the experimental ratio of Y/Y_0, for every Y value, the respective Y_0 value of the same trap depth is determined with the aid of the respective probing energy levels of Y and Y_0. The transition frequency ω_t is determined from the drop of Y to a factor of 2 (vertical line) from the respective light intensity independent value of Y_0 corresponding to the same probing energy level that has for $\omega \cong 1.4\omega_t$.

The experimental ratio of Y/Y_0 is plotted in Fig. 2(a)–(c) (points) as a function of the angular modulation frequency ω for the A state and various light exposed states. It can be seen that in all states, the respective Y/Y_0 has a spectral shape which is indeed in a very good agreement with that of the $H(\omega_t, \omega)$ function (solid line) of Eq. (2). This is also the

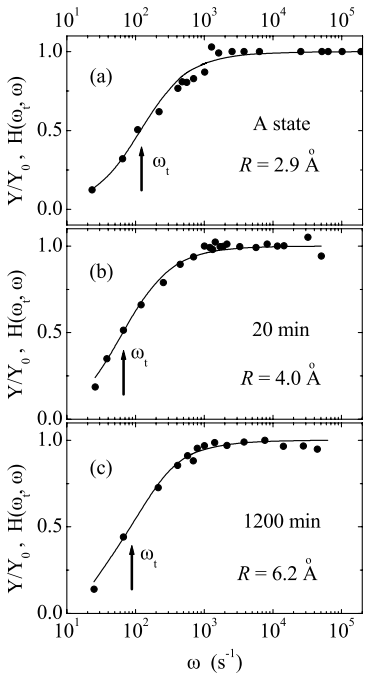

Fig. 2. Experimental ratios of Y/Y_0 (circles) and weighting functions $H(\omega_t, \omega)$ (solid lines) as a function of angular modulation frequency ω of A state in (a) and light exposed states in (b), (c) for the indicated irradiation times. Arrows indicate the respective transition frequency ω_t. The capture radius R of each state is also included.

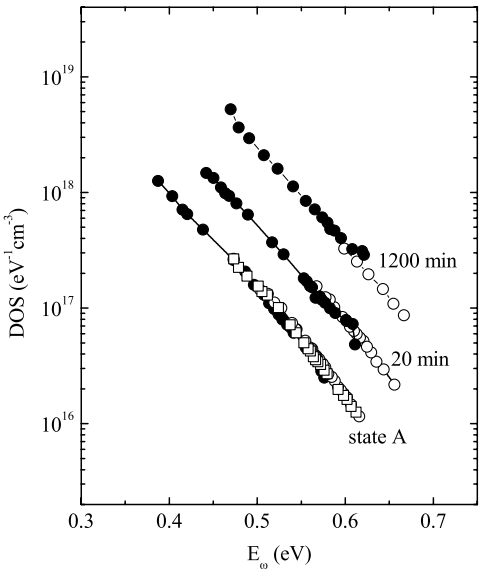

Fig. 3. Calculated DOS from the MPC data in A state and light exposed states for the indicated irradiation times as a function of the probing energy level E_ω. Open and closed symbols correspond to the data measured with the weak (F_0 or F_0') and moderate (F) bias light intensities, respectively.

experimental manifestation of the spectral shape of H function that was recently extracted by theoretical calculations [17].

The absolute DOS, $D(E_\omega)$, was extracted from Eq. (1) by means of the respective MPC data of various bias light intensities and the ratio of c_p/μ as calculated from $c_p/\mu = e\omega_t/\sigma_p$, where σ_p is the dc photoconductivity [17]. The so derived DOS in the A and light exposed states are plotted in Fig. 3. In every state, the $D(E)$ distributions extracted from the data of various bias light intensities fall into a single exponential tail with a characteristic temperature of about $T_0 = 610$ K. This value of T_0 agrees with that obtained from the time of flight measurements [20] suggesting that the valence band-tail is probed. The above value of T_0 also agrees with those obtained from TPC [12] and optical absorption measurements [21].

4. Discussion

From the featureless shape of the DOS of Fig. 3 there is no evidence of light-induced metastable defects at specific energy levels (i.e. VAPs) [1]. The light-induced changes of Fig. 3 could be originated from an increase up to about an order of magnitude in the absolute magnitude of the DOS and/or a parallel shift of the DOS up to 110 meV towards midgap. It is difficult to distinguish between these two possibilities due to the absence of an apparent structure in the shape of the DOS. In general, these changes in the DOS are expected to produce similar changes in the absorption edge with which the photodarkening effect is related. This effect is manifested by a parallel shift of the absorption edge to lower photon energies that is believed to arise from changes in the valence band [1]. However, this shift of the absorption edge is amounted to only about 30 meV in our films and saturates rapidly within about 20 min of illumination [21], while the shift of the DOS is continuous up to 1200 min of illumination (see Fig. 3). Therefore, it is only the initial shift in the DOS, that is about 50 meV and induced during the first 20 min of illumination, that could be connected with the absorption edge shift. The observed relatively stronger shift of the DOS could be produced by other changes. It is worthwhile to notice that the changes in the MPC are only related to changes in the DOS of the valence band side, whereas the changes in the optical absorption are related to changes in the convolution integral of the DOS of valence and conduction band side. However, there is no information about light-induced changes in the DOS of the conduction band side.

In the A state, R was found to be 2.9 Å. The same average capture radius $R = 2.8 \pm 0.3$ Å was also obtained from films prepared in different deposition runs. This value is of the order of the interatomic spacing and more likely corresponds to carriers capture into neutral centers rather than charged defects. The exponential probing trapping centers in a-As_2Se_3 with $R = 2.9$ Å are more likely the neutral traps of the valence band-tail. Since a possible

contribution from charged defects of the VAP model should result in a relatively higher effective R, we conclude that the contribution from such defects is negligible in the A state.

From the indicated values of R in Fig. 2 it can be seen that this parameter increases in the light exposed states reaching a value of $R = 6.2$ Å. Therefore, the changes in the DOS (Fig. 3) upon light irradiation is also accompanied by an increase of R. This suggests that both phenomena are probably related to the same microscopic mechanism. This is also supported by the fact that the above light-induced changes in the DOS and R are removed simultaneously by thermal annealing. The increase of R can be explained with a light-induced structural disorder that is expected to facilitate the carriers capture process.

Information about a light-induced disorder can be obtained from EXAFS experiments. Specifically, Kolobov et al. [22] and Chen et al. [5] from the analysis of the EXAFS measurements performed using unpolarized laser light found earlier that the structural disorder increases during illumination, while after switching off the light a portion of this disorder still persists. In contrast, Chen et al. [23] using polarized laser light in their EXAFS experiments found recently that all the light-induced structural disorder recovers completely after the laser light is turned off. The different behavior in the latter case could be attributed to the use of polarized laser light, which is expected to produce bonding rearrangements preferentially along the polarization direction of the light [23]. Our conclusion that R increases because of a light-induced structural disorder that remains after illumination agrees with the earlier EXAFS measurements [5,22] where unpolarized illumination was used, as in our case.

Although the DOS of Fig. 3 are featureless, the light-induced increase of R could support some creation of charged defects under the band-tail. This possibility is examined using the model calculations of Fig. 4(a)–(c), which demonstrate the sensitivity of our analysis of the imaginary term to resolve additional defect states under the band-tail. Fig. 4(a)–(c) present the ratios of Y/Y_0 which were calculated assuming an exponential valence band tail with $T_0 = 610$ K with a fixed capture coefficient $c_t^t = 1 \times 10^{-7}$ cm^{-3} s^{-1}. Under this tail there is a gaussian distribution of charged defects peaked at 0.35 eV above the valence band edge with a standard deviation of $\sigma = 0.135$ eV and a capture coefficient c_t^d 4–50 times higher than that of the tail states due to their charge state. The defect states always have a relatively small contribution to the imaginary term of about 25%. The Y_0 values are referred to the emission-limited regime by taking that ω_{t0}^t, $\omega_{t0}^d \ll \omega$. The Y values were calculated with a fixed transition frequency ω_t^t for the neutral tail states. The transition frequency ω_t^d for the defect states was defined according to their capture coefficient c_t^d.

Our calculations show that in the cases of Fig. 4(b) and (c), where it is considered $c_p^d/c_p^t \geq 8$ that is reasonable for charged defects, ω_t shifts above ω_t^t due to the contribution of the

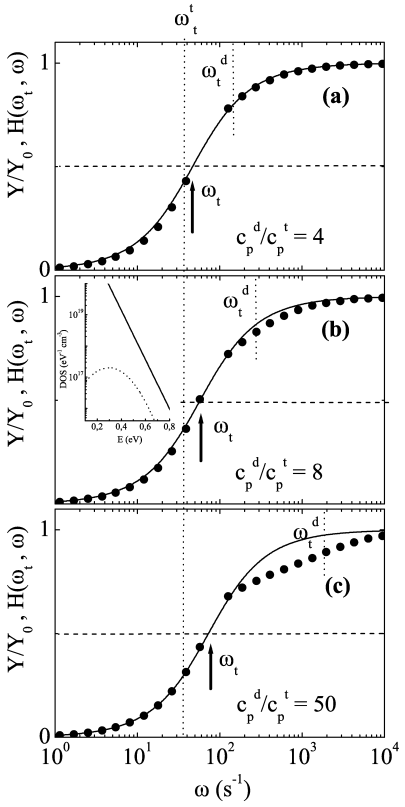

Fig. 4. Calculated ratio of Y/Y_0 (circles) and weighting function $H(\omega_t, \omega)$ (solid lines) as a function of angular modulation frequency ω for the indicated ratios c_p^d/c_p^t. Vertical dotted lines indicate the transition frequencies ω_t^t and ω_t^d, while arrows, the transition frequency ω_t. The inset in (b) indicates the assumed DOS of the valence band tail (solid line) and the defect distribution (dotted line).

defects. From this shift of ω_t it can be deduced a small increase in the effective R that is comparable to that obtained experimentally in the present paper by light irradiation. The respective calculated ratios of Y/Y_0 of the above figures systematically deviate from the respective $H(\omega_t, \omega)$ functions (solid line) near ω_t^d (dashed line) where a second drop of Y is taking place. Therefore, the presence of charged defects under the band-tail can be manifested mainly by the above second drop in the spectra of Y/Y_0. Since such a second drop was not observed in any of the experimental spectra of Fig. 2(a)–(c), it seems unlikely that the light-induced increase in R arises from the light-creation of charged defects under the band-tail. Therefore, a possible contribution to the Y term from these charged defects is negligible.

5. Conclusion

Our analysis of the imaginary term of the MPC in a-As_2Se_3 reveals that the holes interact through trapping and

thermal release with a nearly exponential band tail of neutral trapping states. Upon light irradiation, an increase and/or a reversible parallel shift of the DOS to deeper energies take place. The changes in the DOS were accompanied by a reversible increase in R that attributed to a light-induced structural disorder. The light-induced changes in the DOS and R do not correlate in a straightforward way with the photodarkening effect. A thermal interaction of holes with charged defects of the VAP model was not detected.

References

[1] K. Shimakawa, K. Kolobov, S.R. Elliott, Adv. Phys. 44 (1995) 475.
[2] P.W. Anderson, Phys. Rev. Lett. 34 (1975) 953.
[3] M. Kastner, H. Frtitzsche, Philos. Mag. B 37 (1978) 199.
[4] A.V. Kolobov, H. Oyanagi, K. Tanaka, Ke Tanaka, Phys. Rev. B 55 (1997) 726.
[5] G. Chen, H. Jain, S. Khalid, J. Li, D.A. Drabold, S.R. Elliott, Solid State Commun. 120 (2001) 149.
[6] A.V. Kolobov, H. Oyanagi, A. Roy, K. Tanaka, J. Non-Cryst. Solids 232–234 (1998) 80.
[7] A.V. Kolobov, M. Kondo, H. Oyanagi, R. Durny, A. Matsuda, K. Tanaka, Phys. Rev. B 56 (1997) R485.
[8] K. Tanaka, J. Optoel. Adv. Mater. 3 (2001) 189.
[9] J. Orenstein, M.A. Kastner, V. Vaninov, Philos. Mag. B 46 (1982) 23.
[10] V. Vaninov, J. Orenstein, M.A. Kastner, Philos. Mag. B 45 (1982) 399.
[11] D. Wolverson, R.T. Philips, Philos. Mag. B 57 (1988) 635.
[12] C. Main, D.P. Webb, R. Brüggemann, S. Reynolds, J. Non-Cryst. Solids 137–138 (1991) 951.
[13] P. Kounavis, E. Mytilineou, J. Non-Cryst. Solids 164/166 (1993) 623.
[14] G.J. Adriaenssens, Philos. Mag. B 62 (1990) 79.
[15] G.J. Adriaenssens, A. Stesmans, J. Optoel. Adv. Mater. 4 (2002) 837.
[16] P. Kounavis, J. Non-Cryst. Solids 326–327 (2003) 98.
[17] P. Kounavis, Phys. Rev. B 64 (2001) 45204.
[18] P. Kounavis, Phys. Rev. B 65 (2002) 155207.
[19] P. Kounavis, E. Mytilineou, J. Phys.: Condens. Matter. 11 (1999) 9105.
[20] B. Khan, M.A. Kastner, D. Adler, Solid State Commun. 45 (1983) 187.
[21] P. Kounavis, E. Mytilineou, Philos. Mag. Lett. 72 (1996) 117.
[22] A. Kolobov, H. Oyanagi, A. Roy, K. Tanaka, J. Non-Cryst Solids 227–230 (1998) 710.
[23] G. Chen, H. Jain, M. Vlček, J. Li, D.A. Drabold, S. Khalid, S.R. Elliott, J. Non-Cryst. Solids 326–327 (2003) 257.